

## Superconducting properties of MgCNi<sub>3</sub> films

D. P. Young, M. Moldovan, D. D. Craig, and P. W. Adams

*Department of Physics and Astronomy, Louisiana State University, Baton Rouge, Louisiana 70803, USA*

Julia Y. Chan

*Department of Chemistry, Louisiana State University, Baton Rouge, Louisiana 70803, USA*

(Received 28 April 2003; published 3 July 2003)

We report the magnetotransport properties of thin polycrystalline films of the recently discovered nonoxide perovskite superconductor MgCNi<sub>3</sub>. CNi<sub>3</sub> precursor films were deposited onto sapphire substrates and subsequently exposed to Mg vapor at 700 °C. We report transition temperatures ( $T_c$ ) and critical field values ( $H_{c2}$ ) of MgCNi<sub>3</sub> films ranging in thickness from 7.5 nm to 100 nm. Films thicker than  $\approx 40$  nm have a  $T_c \sim 8$  K, and an upper critical field  $H_{c2}(T=0) = 14$  T, which are both comparable to that of polycrystalline powders. Hall measurements in the normal state give a carrier density,  $n = -4.2 \times 10^{22} \text{ cm}^{-3}$ , that is approximately 4 times that reported for bulk samples.

DOI: 10.1103/PhysRevB.68.020501

PACS number(s): 74.70.Ad, 74.78.-w, 73.50.-h

Over the last decade a broad and significant research effort has emerged aimed at identifying and characterizing relatively low- $T_c$  superconductors that are exotic in their normal state properties and/or order parameter symmetries. Examples include the ternary borocarbides LnNi<sub>2</sub>B<sub>2</sub>C, where Ln is a lanthanide element,<sup>1</sup> the noncopper layered perovskite Sr<sub>2</sub>RuO<sub>4</sub>,<sup>2</sup> and the superconducting itinerant ferromagnets UGe<sub>2</sub> (Ref. 3) and ZrZn<sub>2</sub>.<sup>4</sup> The recently discovered intermetallic MgCNi<sub>3</sub> (Ref. 5) falls into this class in that its major constituent Ni is ferromagnetic, generating speculation that the system may be near a ferromagnetic ground state.<sup>6</sup> In addition, MgCNi<sub>3</sub> is the only known nonoxide perovskite that superconducts, and is thus a compelling analog to the high- $T_c$  perovskites. Notwithstanding the widespread interest in MgCNi<sub>3</sub>, its status as a non-BCS superconductor remains controversial.<sup>7,8</sup> Electron tunneling studies of the density of states in polycrystalline powders have yielded conflicting results as to whether or not MgCNi<sub>3</sub> exhibits a BCS density of states spectrum.<sup>9,10</sup> Tunneling into sintered powders is technically difficult, and indeed, a detailed quantitative characterization of MgCNi<sub>3</sub> has, in part, been hampered by the fact that only polycrystalline powder samples have been available. Obviously, single crystal samples and/or polycrystalline films would be a welcome development both in terms of fundamental research and possible applications. In the present paper we present magnetotransport studies of thin MgCNi<sub>3</sub> films. We show that the transition temperature of the films is only weakly dependent upon film thickness for thicknesses greater than 10 nm, and that both the transition temperature and critical field values of films with thicknesses greater than 40 nm are comparable to that of powder samples synthesized via standard solid state reaction processes.

The MgCNi<sub>3</sub> films were grown by first depositing thin films of the metastable intermetallic CNi<sub>3</sub> onto sapphire substrates by electron-beam evaporation of CNi<sub>3</sub> targets. Typical deposition rates were  $\sim 0.1$  nm/s in a 2  $\mu$ Torr vacuum. All of the evaporations were made at room temperature, and the resulting films were handled in air. The targets consisted of arc-melted buttons of high purity graphite (Johnson Matthey, 99.9999%) and nickel (Johnson Matthey, 99.9999%). The

buttons were made with a starting stoichiometry of CNi<sub>3,25</sub> to compensate for some loss of nickel during the melting process. The CNi<sub>3</sub> structure of the pristine films was verified by x-ray diffraction.<sup>11</sup> Scanning electron microscopy showed the CNi<sub>3</sub> films to be very smooth with no discernible morphological features in 10  $\mu\text{m} \times 10 \mu\text{m}$  micrographs. The films were also quite adherent, and could not be pulled off with Scotch tape.

MgCNi<sub>3</sub> was synthesized by first sealing pristine CNi<sub>3</sub> films in a quartz tube under vacuum with approximately 0.1 g of magnesium metal (Alfa Aesar, 99.98%). The tube was then placed in a furnace at 700 °C for 20 min, after which the entire tube was quenched-cooled to room temperature. X-ray powder diffraction analysis of the magnesiated films verified that MgCNi<sub>3</sub> was formed. Intensity data were collected using a Bruker Advance D8 powder diffractometer at ambient temperature in the  $2\theta$  range between 20° and 60° with a step width of 0.02° and a 6 s count time. The inset of Fig. 1 shows the x-ray diffraction data for a 90 nm film on a sapphire substrate. The powder pattern shows that the film has good crystallinity and that it can be indexed according to the  $Pm\bar{3}m$  space group, with  $a = 0.38070(2)$  nm. The pattern also indicates that the films grew preferentially along the ( $h00$ ) reflections. Electrical resistivity measurements were made by the standard four-probe ac technique at 27 Hz with an excitation current of 0.01 mA. Two-mil platinum wires were attached to the films with silver epoxy, and the measurements were performed in a 9-T Quantum Design PPMS system from 1.8–300 K.

In the main panel of Fig. 1 we plot the resistivity of a 7.5 and a 60 nm film as function of temperature in zero magnetic field. The thickness values refer to that of the CNi<sub>3</sub> layers as determined by a quartz crystal deposition monitor. Subsequent profilometer measurements of the magnesiated films did not show any significant increase in film thickness. We note that the resistance ratio,  $\rho_{290 \text{ K}}/\rho_{10 \text{ K}} \approx 3$  of the 60 nm film, is slightly better than that reported for pressed pellet samples.<sup>5,12</sup> Indeed, the overall shape of the 60 nm curve is very similar to that of MgCNi<sub>3</sub> powders, but the normal state

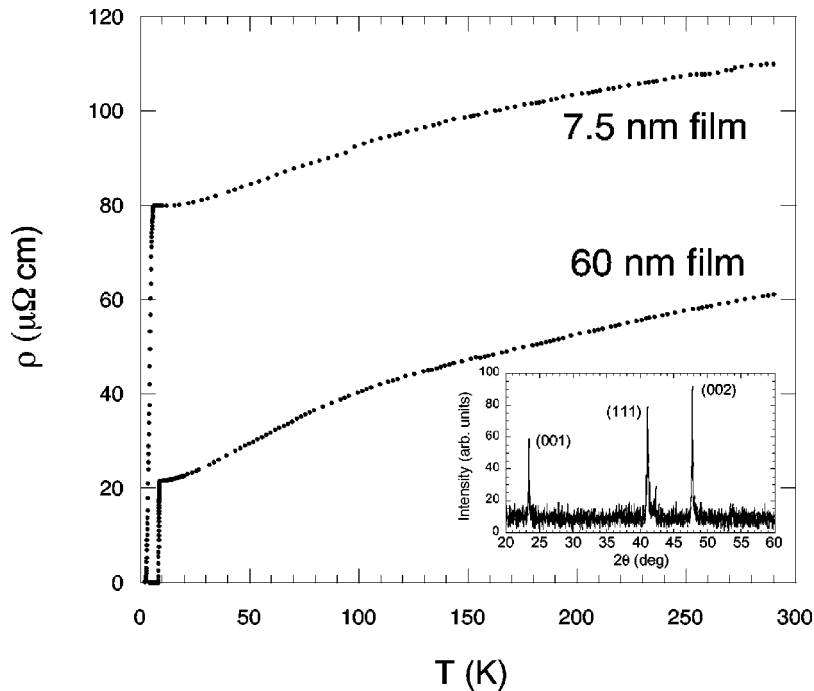


FIG. 1. Resistivity of a 60 nm and a 7.5 nm  $\text{MgCNi}_3$  film as a function of temperature in zero magnetic field. The midpoint transition temperatures of the 60 nm and 7.5 nm films were  $T_c = 8.2$  K and  $T_c = 3.9$  K, respectively. Inset: X-ray powder diffraction pattern of a 90 nm  $\text{MgCNi}_3$  film on sapphire.

resistivity  $\rho_{10\text{K}} \approx 20 \mu\Omega\text{cm}$ , is a factor of 2–6 lower than polycrystalline powder values. The midpoint of the resistive transitions in Fig. 1 are 8.2 and 3.9 K for the 60 and 7.5 nm films, respectively. In Fig. 2 we plot the resistive transitions for a variety of film thicknesses  $d$ . Note that the transition temperature  $T_c$  is relatively insensitive to  $d$  down to about  $d = 15$  nm, below which  $T_c$  is suppressed and broadened.

The perpendicular critical field behavior of a 60 nm film is shown in Fig. 3. As is the case with pressed pellets of  $\text{MgCNi}_3$  powder, the resistive critical field transition width is only weakly temperature dependent.<sup>12</sup> We defined the critical field,  $H_{c2}$ , as the midpoint of the transitions in Fig. 3, and in Fig. 4 we plot critical values as a function of temperature.

The solid symbols represent a 60 nm film, and the open symbols are for a polycrystalline sample from Ref. 12. Clearly the 60 nm critical field behavior is comparable to that of sintered  $\text{MgCNi}_3$  powders, which are known to have an anomalously high critical field and excellent flux pinning properties.<sup>13</sup> The zero temperature critical field can be estimated using the relation<sup>14</sup>  $H_{c2}(0) = -0.693(dH_{c2}/dT)_{T_c} T_c$ . From the data in Fig. 4 we obtain  $(dH_{c2}/dT)_{T_c} = -2.3$  T/K,  $H_{c2}(0) = 12.8$  T and a zero temperature coherence length  $\xi(0) \approx 5$  nm.

We have also made Hall measurements of the films in the normal state between 10 K and room temperature. In the inset of Fig. 4 we show the Hall voltage as a function of

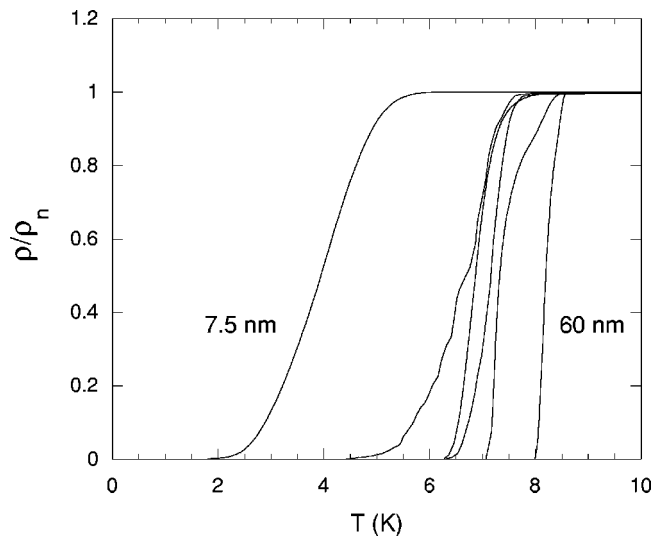


FIG. 2. Resistive transitions for varying film thickness. The curves correspond from left to right to  $\text{MgCNi}_3$  layer thicknesses of 7.5, 15, 30, 45, and 60 nm.

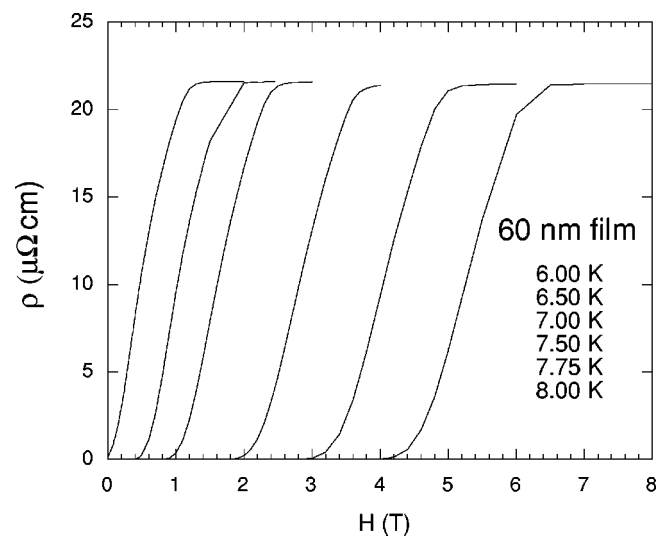


FIG. 3. Resistive critical field transitions of a 60 nm film at different temperatures. The magnetic field was applied perpendicular to the film surface.

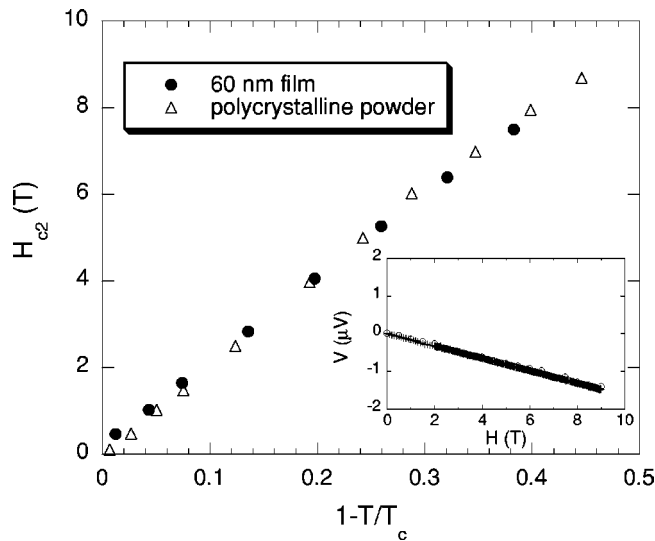


FIG. 4. Upper critical field values of the 60 nm film of Fig. 3 (solid symbols) and a polycrystalline sample (open symbols) from Ref. 12 as a function of reduced temperature. Inset: Hall voltage of a 90 nm  $\text{MgCNi}_3$  film using a 0.1 mA probe current at 10 K (crosses) and 200 K (circles). The solid lines are linear least-squares fits to the data. The low temperature data correspond to a carrier density of  $n = -4.2 \times 10^{22} \text{ cm}^{-3}$ .

magnetic field at 10 and 200 K. The solid lines are linear fits to the data. The slopes of the lines are proportional to the Hall coefficient  $R_H = 1/en$ , where  $n$  is the effective carrier density. Clearly the  $\text{MgCNi}_3$  films have electronlike carriers as is the case in the bulk material. However, the calculated carrier density at 10 K,  $n = -4.2 \times 10^{22} \text{ cm}^{-3}$ , is about 4 times larger than that reported in Ref. 12 for sintered powder samples. It is somewhat surprising that the superconducting properties of the films are so similar to that of the bulk systems given the large enhancement in the density of states suggested by the Hall data.

Interestingly, recent studies of Ni-site substitution with Co, which in principle hole dopes the system, show a rapid

quenching of the superconducting phase with increasing Co concentration,<sup>15</sup> even for concentrations as little as a few percent. Two possible explanations for this sensitivity to Co doping immediately come to mind. One is that Co behaves as a localized magnetic impurity and consequently produces pair breaking.<sup>16</sup> However, susceptibility measurements of  $\text{MgCNi}_{3-x}\text{Co}_x$  powders are not consistent with what would be expected for free Co moments. Furthermore, even at doping levels up to  $x=0.75$  no long range magnetic order is seen.<sup>15</sup> A second possibility is that superconductivity in  $\text{MgCNi}_3$  is very sensitive to a narrow spectral feature in the electronic structure,<sup>17</sup> and that at even small Co doping levels the optimum band filling is compromised. Our Hall data, however, would suggest that this is not case and that  $T_c$  is not extraordinarily sensitive to the density of states. Presumably, the enhancement we observe in the Hall carrier density reflects a significant modification of bands near the Fermi surface that is a result of disorder or perhaps substrate-induced strain.

In conclusion, we report the first synthesis of  $\text{MgCNi}_3$  films and find that their transition temperatures and critical field behavior are very similar to that of bulk powder samples. The films are smooth, adherent, and show no significant air sensitivity. A thin film geometry lends itself quite well to planar counter-electrode tunnelling measurements of the electronic density states, thus providing a compelling alternative to scanning electron microscopy tunneling. Such a study in  $\text{MgCNi}_3$  films should prove invaluable in resolving the nature of the superconducting condensate. The film geometry will also allow access to the spin paramagnetic limit in parallel magnetic field studies, as well as possible electric field modulation of the carrier density via gating and critical current studies.

We gratefully acknowledge discussions with Dana Browne, Phil Sprunger, and Richard Kurtz. This work was supported by the National Science Foundation under Grant DMR 01-03892. We also acknowledge support of the Louisiana Education Quality Support Fund under Grant No. 2001-04-RD-A-11.

<sup>1</sup>R.J. Cava *et al.*, Nature (London) **367**, 252 (1994); R.J. Cava *et al.*, Physica C **235**, 154 (1994).

<sup>2</sup>Y. Maeno *et al.*, Nature (London) **372**, 532 (1994); Y. Sidis *et al.*, Phys. Rev. Lett. **83**, 3320 (1999).

<sup>3</sup>S. Saxena *et al.*, Nature (London) **406**, 587 (2000).

<sup>4</sup>C. Pfleiderer *et al.*, Nature (London) **412**, 58 (2001).

<sup>5</sup>T. He *et al.*, Nature (London) **410**, 63 (2001).

<sup>6</sup>H. Rosner, R. Weht, M.D. Johannes, W.E. Pickett, and E. Tosatti, Phys. Rev. Lett. **88**, 027001 (2002).

<sup>7</sup>J.Y. Lin *et al.*, Phys. Rev. B **67**, 052501 (2003).

<sup>8</sup>K. Voelker and M. Sigrist, cond-mat/0208367 (unpublished).

<sup>9</sup>Z.Q. Mao *et al.*, Phys. Rev. B **67**, 094502 (2003).

<sup>10</sup>G. Kinoda, M. Nishiyama, Y. Zhao, M. Murakami, N. Koshizuka,

and T. Hasegawa, Jpn. J. Appl. Phys. **40**, L1365 (2001).

<sup>11</sup>P. Villars and L.D. Calvert, *Pearson's Handbook of Crystallographic Data for Intermetallic Phases*, 2nd ed. (ASM International, Materials Park, OH, 1991), Vol. 2.

<sup>12</sup>S.Y. Li *et al.*, Phys. Rev. B **64**, 132505 (2001).

<sup>13</sup>L.D. Cooley *et al.*, Phys. Rev. B **65**, 214518 (2002).

<sup>14</sup>N.R. Werthamer, E. Helfand, and P.C. Hohenberg, Phys. Rev. **147**, 295 (1966).

<sup>15</sup>M.A. Hayward *et al.*, Solid State Commun. **119**, 491 (2001).

<sup>16</sup>M. Tinkam, *Introduction to Superconductivity* (McGraw-Hill, New York, 1996).

<sup>17</sup>J.H. Shim, S.K. Kwon, and B.I. Min, Phys. Rev. B **64**, 180510(R) (2001).